Molecular Diversity (2018) 22:827–840
https://doi.org/10.1007/s11030-018-9832-5

ORIGINAL ARTICLE

Synthesis, docking and anticancer activity of azo-linked hybrids of 1,3,4-thia-/oxadiazoles with cyclic imides

Priyanka Bhatt[1] · **Manoj Kumar**[2] · **Anjali Jha**[1]

Received: 1 January 2018 / Accepted: 14 May 2018 / Published online: 8 June 2018

Abstract

A series of novel analogues based on a diazole-imide pharmacophore were synthesized by diazotizing substituted 1,3,4-thia-/oxadiazol-2-amines and subsequently coupling the resulting diazonium salts with *N*-substituted cyclic imides. The resulting compounds **C1** to **C28** were characterized by various spectral methods, *viz.* IR, NMR and mass spectroscopy. All the synthesized compounds were tested against two human cancer cell lines: human breast adenocarcinoma cell line MCF-7 and colorectal adenocarcinoma cell line HT-29. Among the synthesized compounds, **C14** (2-(4-chloro-3-((5-(4-nitrophenyl)-1,3,4-thiadiazol-2-yl)diazenyl)phenyl)-4,5,6,7-tetrahydro-1*H*-isoindole-1,3(2*H*)-dione) emerged as a potential candidate against both MCF-7 and HT-29 with IC_{50} values of 0.09 ± 0.02 μM and 0.11 ± 0.03 μM, respectively. Similarly, compound **C16** displayed highest anticancer activity against MCF-7 cell line with IC_{50} = 0.07 ± 0.02 μM. Target fishing (inverse docking) using ChemMapper server identified EGFR tyrosine and CDK2 kinases as high priority targets for this pharmacophore. Computational docking (AutoDock 4.2) was used to analyse the interactions between the target proteins and active compounds.

Graphical Abstract

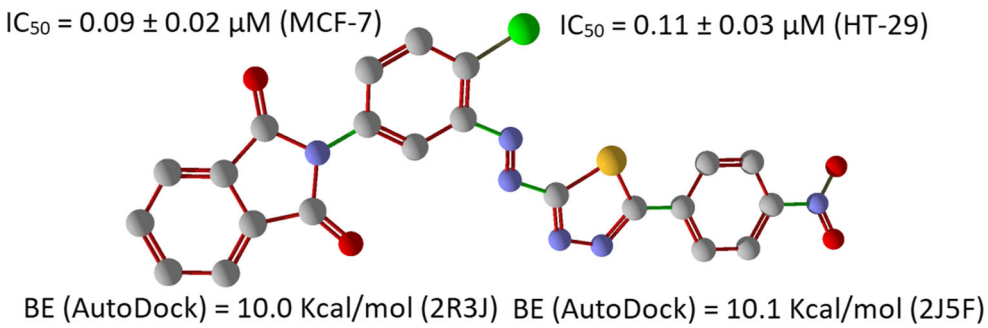

Keywords Thiadiazoles · Oxadiazoles · Anticancer activity · ChemMapper · AutoDock · Docking

Introduction

Cancer has been a major health problem with millions of reported death annually. It also affects the socio-economical fabric of society [1,2]. Chemotherapy, which is one of the first-line strategies in cancer treatment, heavily relies on cytotoxic and antineoplastic drugs. Despite several serious efforts, today's medications are far from perfect with very low efficacy and high side effects. Many of these drugs are also very expensive, making them unaffordable to the general public [3–7].

Electronic supplementary material The online version of this article (https://doi.org/10.1007/s11030-018-9832-5) contains supplementary material, which is available to authorized users.

✉ Anjali Jha
anjalimanishjha@yahoo.com

[1] Department of Chemistry, GIS, GITAM University, Rushikonda, Visakhapatnam 530045, India

[2] Department of Chemistry, Indian Institute of Technology Roorkee, Roorkee 247667, India

This problem may have twofold solutions. First, decipher the functioning of the tumour cell and study the reasons/agents/factors which trigger its uncontrolled proliferation [8,9]. This piece of information will help navigate more biologically important space of the tumour cell, and new targets can be discovered. The second and more immediate solution is the diversification of the existing drug arsenal and discovery of new drugs based on novel chemotypes (termed as novel chemical entities, NCEs) [10]. In the quest of NCEs, the concept of hybrid pharmacophore can be a promising approach [11]. In a hybrid molecule two or more distinct pharmacophore domains are connected together by a suitable linker. Each component part has its own biological space, and by combining them, the final pharmacophore may show enhanced and/or novel pharmacological effects [11]. Other factors such as potency, selectivity, metabolism and half-life ($t_{1/2}$) of the hybrid molecule may be different from its structural components. The use of drugs based on single hybrid molecule as compare to the co-formulation of two different components (or drugs) may be synthetically cost-effective. This concept of hybrid pharmacophore (also called covalent biotherapy) has been successfully employed in many previous drug discovery efforts [12–17].

Inspired by the above facts, we have designed a series of novel azo-linked hybrids of 1,3,4-thia-/oxadiazoles with cyclic imides. The facile construction of these analogues was achieved by the initial diazotization of five-member thia-/oxadiazoles-2-amines followed by condensation of the resulting diazonium salt with suitable *N*-substituted cyclic imides. Both components of the hybrid *viz.* thia-/oxadiazoles and cyclic imides are biologically active of their own accord [18–22]. In fact, cyclic imides (and their derivatives) form the structural framework of many known anticancer drugs such as rebeccamycin, granulaimide, camphorataimide B and showdomycin. Both moieties were linked together by an azo group (–N=N–). The azo linkage was selected because of its low reactivity and easy accessibility by simple diazotization.

A small library of 28 compounds (**C1–C28**) was constructed and tested against two cancer cell lines: human breast adenocarcinoma cell line MCF-7 and colorectal adenocarcinoma cell line HT-29 by MTT assay. Compound **C14** displayed higher anticancer activity in the series against both the cancer cell lines. ChemMapper server [23] was used to screen the Protein Data Bank (www.rcsb.org) in inverse docking [24] against both thia-/oxadiazole-based pharmacophores. Two well-validated targets used in the cancer therapy: EGFR tyrosine kinase and CDK2 kinase, displayed high scores [25–29]. AutoDock 4.2 [30] was used to dock our hybrid molecules in the binding site (determined by the coordinates of cognate inhibitors in the respective pdb structures) of both the proteins, and finally, all important interactions were visually inspected using Discovery Studio Visualizer (DSV) and Molegro Molecular Viewer (MMV) [31,32].

Results and discussion

Chemistry

Acid-catalysed condensation of phthalic anhydride or maleic anhydride with suitably substituted amines afforded the corresponding cyclic imides (**1-4**). Reaction proceeds through two consecutive condensations with an amide intermediate. In a separate step, substituted 1,3,4-thia-/oxadiazol-2-amines were diazotized using nitrous acid, followed by azo coupling with the relatively electron-rich site of phenyl ring of imides (**1-4**) (Scheme 1). Library of synthesized compounds **C1-C28** is presented in Table 1.

Spectral analysis

The structures of all the synthesized compounds **C1–C28** were confirmed using various spectral techniques such as FT-IR, ^{1}HNMR, ^{13}CNMR, HMRS, and data were in full agreement with the proposed structures (see supporting information). The IR spectra of the compounds (**C1-C28)** displayed two sets of intense signals at 1765, 1715 cm^{-1} and another at 1762, 1710 cm^{-1} that can be attributed to the two carbonyl groups of the *N*-phenylphthalimide and *N*-phenylmaleimide ring, respectively. The other major signals observed in the IR of these compounds were ~1610–1602; 1585–1550; 1445–1420; and 1385–1340 cm^{-1} and could be assigned to υ(C=N); υ(C=C); υ(N=N); and υ(C–C), respectively. The disappearance of the $\upsilon(NH_2)$ signal at ~3200-3310 cm^{-1} and the presence of a signal at ~1445–1420 cm^{-1} clearly indicated that the amino groups of azoles were diazotized and coupled with *N*-phenylphthalimide and *N*-phenylmaleimide to give the targeted compounds, which was further supported by the respective NMR spectra. The IR spectra of the compounds **C9–C12** and **C21–C24** displayed a broad signal in the region 3430–3410 cm^{-1}, which indicates the presence of a hydroxyl (–OH) group, while in compounds **C13–C16** and **C25–C28** two strong signals at ~1540, 1345 cm^{-1} could be attributed to the nitro group of the azole moieties.

The observed ^{1}H and ^{13}CNMR spectra were consistent with the expected structure of the synthesized compounds (**C1–C28)**. The singlet proton signal at δ 1.95–2.50 ppm was due to the methyl group of the thiadiazole ring in the compounds **C1–C4**. Different signals at δ 7.52–8.07 ppm could be attributed to various aromatic protons. Another singlet signal in the range of δ 3.50–4.20 ppm in compounds **C9–C12** and **C21–C24** could be assigned to the OH proton of the 4-hydroxyphenyl group.

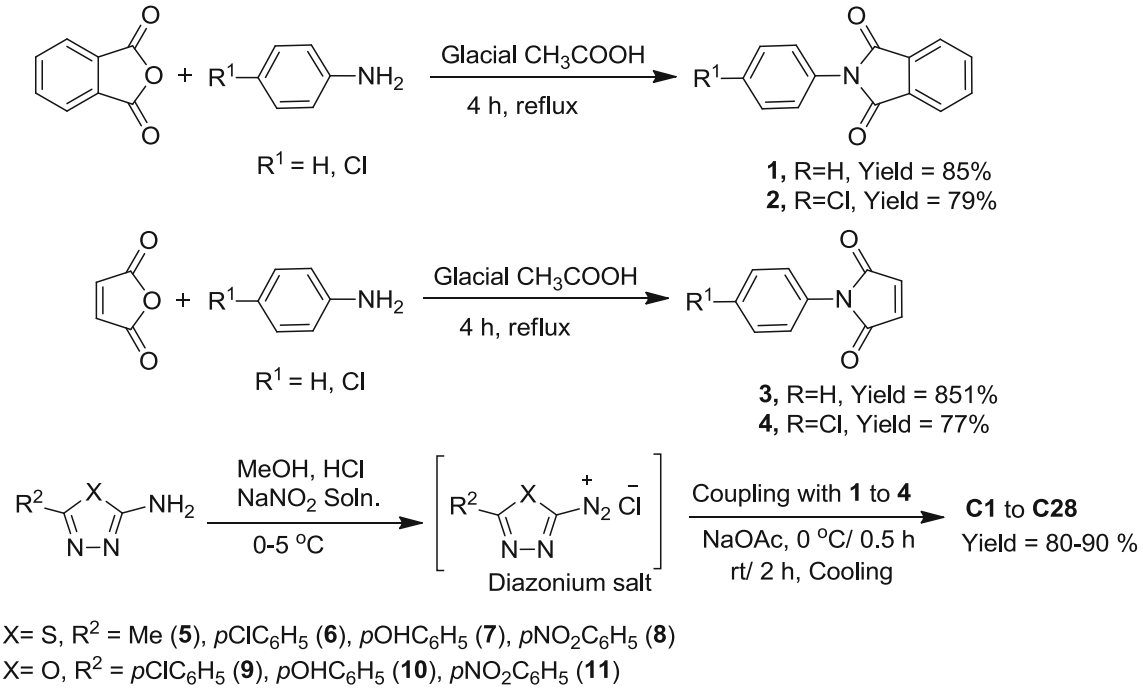

Scheme 1 Synthesis of compounds **C1** to **C28**

Table 1 Structural diversity of synthesized hybrids of 1,3,4-thia-/oxadiazoles with cyclic imides

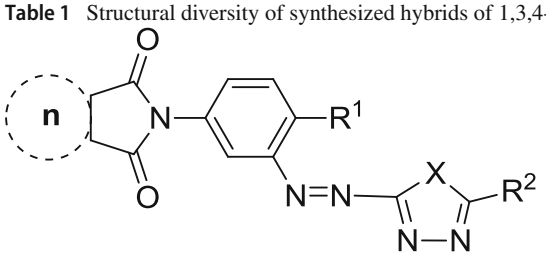

C1	*n* = Ph, X = S, R^1= H, R^2= CH_3	**C15**	*n* = 0, X = S, R^1= H, R^2= NO_2
C2	*n* = Ph, X = S, R^1= Cl, R^2= CH_3	**C16**	*n* = 0, X = S, R^1= Cl, R^2= NO_2
C3	*n* = 0, X = S, R^1= H, R^2= CH_3	**C17**	*n* = Ph, X = O, R^1= H, R^2= Cl
C4	*n* = 0, X = S, R^1= Cl, R^2= CH_3	**C18**	*n* = Ph, X = O, R^1= Cl, R^2= Cl
C5	*n* = Ph, X = S, R^1= H, R^2= Cl	**C19**	*n* = 0, X= O, R^1= H, R^2= Cl
C6	*n* = Ph, X = S, R^1= Cl, R^2= Cl	**C20**	*n* = 0, X= O, R^1= Cl, R^2= Cl
C7	*n* = 0, X = S, R^1= H, R^2= Cl	**C21**	*n* = Ph, X = O, R^1= H, R^2= OH
C8	*n* = 0, X = S, R^1= Cl, R^2= Cl	**C22**	*n* = Ph, X = O, R^1= Cl, R^2= OH
C9	*n* = Ph, X = S, R^1= H, R^2= OH	**C23**	*n* = 0, X = O, R^1= H, R^2= OH
C10	*n* = Ph, X = S, R^1= Cl, R^2= OH	**C24**	*n* = 0, X = O, R^1= Cl, R^2= OH
C11	*n* = 0, X = S, R^1= H, R^2= OH	**C25**	*n* = Ph, X = O, R^1= H, R^2= NO_2
C12	*n* = 0, X = S, R^1= Cl, R^2= OH	**C26**	*n* = Ph, X = O, R^1= Cl, R^2= NO_2
C13	*n* = Ph, X = S, R^1= H, R^2= NO_2	**C27**	*n* = 0, X = O, R^1= H, R^2= NO_2
C14	*n* = Ph, X = S, R^1= Cl, R^2= NO_2	**C28**	*n* = 0, X = O, R^1= Cl, R^2= NO_2

In the ^{13}CNMR, the signal at δ 164.02–178.01 ppm was due to the carbonyl (C=O) carbon present in the imides. The structures of the all novel synthesized compounds **(C1–C28)** were also confirmed by their high-resolution mass spectrum (HRMS). The ESI-MS spectra displayed a molecular ion signal at $[(M+Na)]^+$ in positive mode. The chemical structures of all the synthesized compounds are shown in Table 1.

Cytotoxicity studies

In vitro cytotoxicity studies were carried out against two human cancer cell lines: breast cancer (MCF-7) and colorectal cancer (HT-29). Doxorubicin (DOX) and 5-fluorouracil (5-FU) were used as a reference drugs for comparison purpose. Some important observations are summarized below (Table 2):

(1) Barring **C21** to **C24**, all the synthesized compounds displayed good to moderate anticancer activity.
(2) With few exceptions, compounds with thiadiazoles moiety (**C5** to **C16**) showed higher cytotoxicity than their respective oxygen analogues (**C17** to **C28**) against both cancer cell lines. For example, **C5** versus **C17**, **C6** versus **C18**, **C7** versus **C19**, and so on.
(3) Compound **C14** (2-(4-chloro-3-((5-(4-nitrophenyl)-1,3,4-thiadiazol-2-yl)diazenyl)phenyl)-4,5,6,7-tetrahydro-1*H*-isoindole-1,3(2*H*)-dione) exhibited excellent anticancer activity with IC_{50} values of 0.09 ± 0.02 μM (MCF-7) and 0.11 ± 0.03 μM (HT-29). Surprisingly, its oxygen analogue **C26** was not so potent. Similarly, compound **C16** displayed highest anticancer activity against MCF-7 cell line with $IC_{50} = 0.07 \pm 0.02$ μM.
(4) Substitution of 4-nitrophenyl group attached to diazole ring by phenyl, 4-chlorophenyl, and 4-hydroxyphenyl groups has a diminishing effect on the cytotoxicity. This inspection is particularly true for thiadiazole-containing compounds.
(5) In general, compounds with phthalimide ring displayed slightly higher activity than respective compounds with maleimide ring. For example, **C1** versus **C3**, **C2** versus **C4**, **C5** versus**C7**, and so on.
(6) One important observation was the low activities of compounds **C21** to **C24**. One common structural feature of all these compounds is the presence of 4-hydroxyphenyl group in oxadiazoles ring.

So in general terms compounds with phthalimide ring, thiadiazole moiety and 4-nitrophenyl group (attached to diazole ring) displayed higher cytotoxicity than compounds with alternative structure features (maleimide ring, oxadiazoles moiety and 4-chloro/4-hydroxyphenyl group attached to diazole ring).

Molecular docking studies

In order to understand the experimental findings (activity data) at molecular level, molecular modelling experiments were performed. ChemMapper was used for computational identification of possible target(s). This server is based on 3D similarity search of the user-provided input with the database of known inhibitors (SHAFTS method). Two proteins 2R3J and 2J5F were among the top scorers (3rd and 7th places, respectively) with previous literature precedents being used as a target in cancer therapy. 2R3J is a cyclin-dependent kinase 2 (CDK2) and plays a key role in mammalian cell cycle. Inhibition of CDK2 can trigger apoptosis (cell death) in tumour/cancer cell with some reversible change in normal cell. Hence, by inhibiting this protein, cancer cell can be selectively targeted. 2J5F is a crystal structure of EGFR kinase domain in complex with an irreversible inhibitor 34-jab. This protein is also a key element of signal transduction pathway. Both the target proteins are important for maintaining the genomic integrity of the cell.

In control docking (or self-docking) experiment, the root-mean-square deviation (RMSD) between the coordinate of cognate ligands and re-docked ligands was found to be 1.1Å (2R3J; 3-bromo-5-phenyl-N-(pyridin-3-ylmethyl)pyrazolo [1,5-*a*]pyrimidin-7-amine) and 0.9Å (2J5F; *N*-[4-(3-bromophenylamino)-quinazolin-6-yl]-acrylamide). This result (< 2Å) indicated that our docking engine is good enough for predicting the native poses.

Drug-likeness of the synthesized compounds was also computationally determined using some online tools. Based on various literature sources following criteria were set for optimal drug-/lead-like behaviour [33–35]:

Molecular weight < 500 dalton; log P (octanol/water) < 5; maximum no. of rings (n_{ring}) ≤ 5; maximum no. of non-terminal single bonds (n_{ntsb}) < 10; maximum no. of hydrogen bond donors (n_{HBD}) < 5; maximum no. of hydrogen bond acceptors (n_{HBA}) < 10; ligand efficiency (LE) ≥ 0.30 kcal/mol/non-hydrogen atoms.

Molecular properties of the synthesized compounds covered the following span:

Molecular weight = 300–380 dalton; log P (octanol/water) = 1.85–7.12; maximum no. of rings (n_{ring}) = 3 − 5; maximum no. of non-terminal single bonds (n_{ntsb}) = 3 − 5; maximum no. of hydrogen bond donors (n_{HBD}) = 0 − 1; maximum no. of hydrogen bond acceptors (n_{HBA})7 − 11; ligand efficiency (LE, 2R3J) = − 0.27 to − 0.42 kcal/mol/non-hydrogen atoms. Ligand efficiency (LE, 2J5F) = − 0.23 to − 0.43 kcal/mol/non-hydrogen atoms.

The predicted oral absorption of the synthesized compounds ranged from 57.75 % to 78.09 % with total polar surface area of 89.6–148.6 Å^2. The synthesized compounds displayed satisfactory range of molecular properties with the possibility of further improvement. Higher potency, good lig-

Table 2 IC_{50} of tested compounds for antitumor screening against MCF-7 and HT-29 cancer cells

Compds	Cytotoxic activity IC_{50}*(μM)		Compds	Cytotoxic activity IC_{50}*(μM)	
	MCF-7	HT-29		MCF-7	HT-29
C1	0.22 ± 0.08	0.31 ± 0.25	C15	0.56 ± 0.28	0.21 ± 0.07
C2	0.91 ± 0.28	0.40 ± 0.12	**C16**	**0.07 ± 0.02**	1.08 ± 0.43
C3	0.83 ± 0.42	0.51 ± 0.06	C17	0.35 ± 0.11	1.36 ± 1.12
C4	1.67 ± 0.72	0.92 ± 0.49	C18	1.32 ± 0.53	0.68 ± 0.36
C5	0.18 ± 0.06	0.60 ± 0.09	C19	0.75 ± 0.15	>10
C6	0.50 ± 0.11	0.38 ± 0.98	C20	2.01 ± 0.83	1.62 ± 0.63
C7	0.23 ± 0.14	3.55 ± 2.52	C21	1.87 ± 1.00	2.50 ± 0.90
C8	0.74 ± 0.19	0.70 ± 0.26	C22	>10	>10
C9	0.13 ± 0.08	0.60 ± 0.26	C23	3.69 ± 0.84	>10
C10	2.59 ± 0.39	0.61 ± 0.12	C24	>10	>10
C11	1.11 ± 0.57	>10	C25	0.49 ± 0.48	5.02 ± 2.51
C12	3.04 ± 1.71	2.03 ± 1.87	C26	0.70 ± 0.37	3.10 ± 0.53
C13	0.25 ± 0.13	0.49 ± 0.28	C27	0.28 ± 0.22	2.05 ± 1.45
C14	**0.09 ± 0.02**	**0.11 ± 0.03**	C28	>10	0.20 ± 0.11
DOX [25]	3.24 ± 0.15	3.75 ± 0.14	5-FU [25]	1.86 ± 0.06	2.16 ± 0.07

Best results are shown in bold

*IC_{50} values indicate the effective concentration of a compound required to achieve 50% growth inhibition. Doxorubicin (DOX) and 5-fluorouracil (5-FU) were used as reference drugs

Table 3 Molecular docking results of the **C14** against target proteins 2R3J and 2J5F

PDB id	Binding energy (AutoDock) Kcal/mol	Hydrophobic residues within 5 Å distance	Hydrogen bond			
			No. of hydrogen bonds	Interacting residues	Bond energy[a] (Kcal/mol)	Bond length Å
2R3J	− 10.0	Ile10, Val18, Ala31, Leu83, Phe92, Leu134, Ala144, Leu298	1	Asp145	− 0.912	3.32
2J5F	− 10.1	Leu718, Phe723, Val726, Ala743, Leu792, Met793, Cys797, Arg841, Leu844, Gln791, Gly793	1	Thr854	− 2.49	2.99

[a]Hydrogen bonding (Energy) between protein and ligand was calculated by PLP (piecewise linear potential) concept

and efficiency, adequate functionality and acceptable range of molecular properties for drug-/lead-like behaviour make these scaffolds a good starting point for further screening exercise (see supporting information for more details).

Computational binding energies ($-\Delta G_{AutoDock}$) determined by AutoDock 4.2 are presented in Table S1 and S2 of the supporting information. From the table, it is obvious that most of the compounds displayed good potencies with $-\Delta G_{AutoDock} \geq 8.0$ Kcal/mol. Compound **C14** which displayed excellent anticancer activity against both the cell lines, also scored well in docking with $-\Delta G_{AutoDock} = -10.0$ Kcal/mol (2R3J) and -10.1 Kcal/mol (2J5F) (Table 3). The binding interactions between this compound and both the proteins were studied and visually inspected using MMV and DSV. Docked pose of **C14** (in 2R3J) was surrounded by a partially hydrophobic cavity with amino acid residues such as Leu718, Phe723, Val726, Ala743, Leu792, Met793, Cys797, Arg841, Leu844, Gln791 and Gly793. A hydrogen bond interaction between C1 and Asp145 was also observed (Fig. 1). Similarly, **C14** also occupied the partially

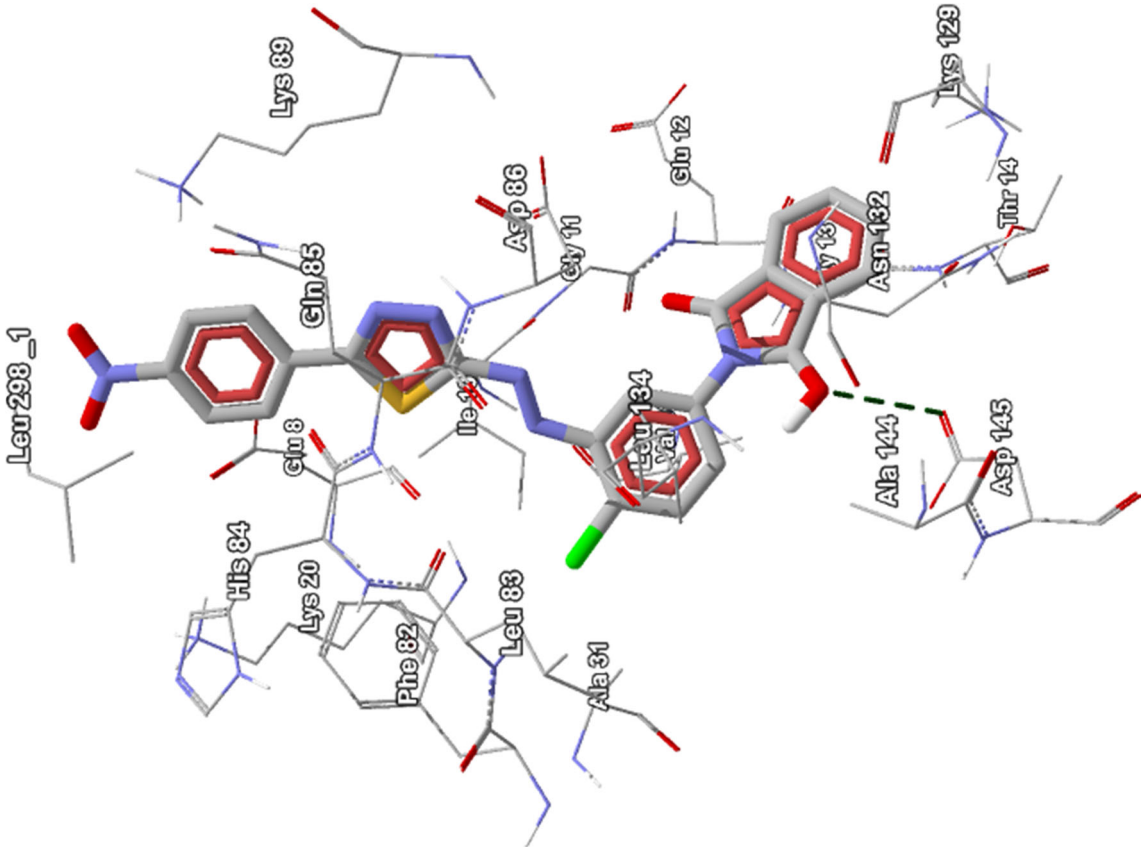

Fig. 1 Position of neighbouring residues around C14 in the binding cavity of 2R3J; hydrogen bond interaction between ligand and Asp145 is shown in dotted (green) line. (Color figure online)

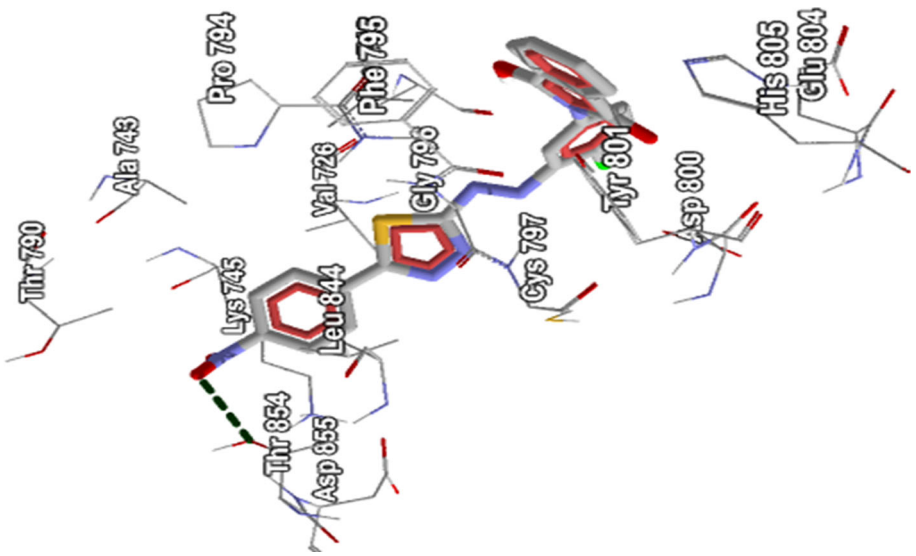

Fig. 2 Position of neighbouring residues around C14 in the binding cavity of 2J3F; hydrogen bond interaction between ligand and Thr854 is shown in dotted (green) line. (Color figure online)

hydrophobic site of 2J5F binding cavity lined up with residues like Leu718, Phe723, Val726, Ala743, Leu792, Met793, Cys797, Arg841, Leu844, Gln791 and Gly793. Oxygen atom of 4-nitrophenyl group (attached to thiadiazole ring) hydrogen bonded to Thr854 (Fig. 2). Details of binding interactions with some other important candidates including neighbouring hydrophobic residues, hydrogen bonds, etc., can be found in the electronic supporting information (ESI). Asp145 (2R3J) and Thr854 (2J5F) were very common amino acids in hydrogen bonding interactions and seemed to have an important role in maintaining the special pose of the docked ligand. Overall, these results provide a worthy explanation for the observed inhibitory activity of the synthesized compounds.

Conclusion

Twenty-eight functionalized derivatives based on thia-/oxadiazoles-imide hybrid pharmacophores were synthesized. MTT-based screening assays against two cancer cell lines MCF-7 (breast cancer) and HT-29 (colorectal cancer) revealed some important structure activity trends. Compounds with phthalimide ring, thiadiazole moiety and 4-nitrophenyl group (attached to diazole ring) displayed higher activity than the compounds with alternative structure features (*viz.* maleimide ring, oxadiazoles moiety and 4-hydroxyphenyl group). Compound **C14** (2-(4-chloro-3-((5-(4-nitrophenyl)-1,3,4-thiadiazol-2-yl)diazenyl)phenyl)-4,5,6,7-tetrahydro-1*H*-isoindole-1,3(2*H*)-dione) displayed significant anticancer activity against both cell lines with IC_{50} values of $0.09 \pm 0.02\ \mu M$ (MCF-7) and $0.11 \pm 0.03\ \mu M$ (HT-29). Computational modelling based on ChemMapper and AutoDock 4.2 was used to get insight at molecular level. Asp145 (2R3J) and Thr854 (2J5F) were very common amino acids in hydrogen bonding interactions and thus seemed to be important in maintaining the lowest energy pose of the ligands in binding cavity. Similar studies based on some other hybrid pharmacophores are currently underway in our laboratory and will be reported in future.

Experimental

Materials and methods

Reagents such as phthalic anhydride, maleic anhydride, aniline, *p*-chloroaniline, acetic anhydride and anhydrous sodium acetate were purchased from Acros Organics® and used as received. All the solvents (high purity, > 98.5%) were distilled prior to use. Melting points were determined using Ambassador® and digital melting point apparatus (Nutronics), Popular India. The solid IR spectra and electronic spectra of the compounds were recorded in KBr and DMSO on Perkin Elmer FT-IR and Perkin Elmer-Spectrum-Lambda-25 spectrophotometer, respectively, at Instrumental Facility, GITAM University, Visakhapatnam. ^{1}H and ^{13}CNMR spectra were obtained using Bruker 400 MHz NMR facility at Institute Instrumentation Centre (IIC), IIT Roorkee, Roorkee. Chemical shift values were reported in parts per million (ppm) using TMS as an internal standard and DMSO-d_6 as NMR solvents. Mass spectrometry data (HRMS) were obtained using a Bruker Daltonics micrOTOF-QII® spectrometer using ESI ionization, with less than 5 ppm error for all HRMS analyses.

Synthetic procedure

Synthesis of N-Phenylphthalimide 1

In a 25-mL round-bottom flask aniline (10.0 mmol, 0.91 mL) and phthalic anhydride (8.0 mmol, 1.184 g) were mixed together in glacial acetic acid (6.0 mL). This reaction mixture was heated to reflux for about 4 h with continuous stirring. The homogenous solution thus formed was cooled to room temperature and then poured into the crushed ice. The resultant precipitate was filtered, washed (with ice-cooled water) and recrystallized from 95% ethanol (rectified spirit). The structure of the product was confirmed by ^{1}HNMR, and data were found in agreement with the previous report [36,37] (Scheme 1).

Compounds **2**, **3** and **4** were synthesized in the similar manner.

Synthesis of C1

To a solution of 5-methyl-1,3,4-thiadiazol-2-amine **5** (1.0 mmol, 0.1151 g) in methanol (2.0 mL) was added conc. HCl (37%, 1.0 mL) followed by addition of 1.0 mL of water (solution A). A freshly prepared cold solution of $NaNO_2$ (0.7 gm/10.0 mL of dist. water, 1.0 mL, solution B) was added slowly and dropwise to the methanolic solution of amine (solution A). The temperature of the system was maintained between 0 and 5 °C (ice-water-cooled bath) during addition and thereafter. An ethanolic solution (5.0 mL) of *N*-phenylphthalimide (1.0 mmol, 0.223 g) and equimolar amount of NaOAc was added slowly with continuous stirring. After complete addition, reaction mixture was first stirred at temperature of ice bath for 30 min and then at room temperature for 2 h. The reaction mixture was transferred to refrigerator for overnight. The solidified product (brownish red) was filtered, washed (cool water) and then recrystallized from ethanol (Scheme 1).

Compounds **C2** to **C28** (Table 1) were prepared by similar procedure with yield ranging between 80 and 90%.

Spectral data

C1. 2-(3-((5-methyl-1,3,4-thiadiazol-2-yl)diazenyl)phenyl)-4,5,6,7-tetrahydro-1*H*-isoindole-1,3(*2H*)-*d*ione

Yield 89%, Grey powder, mp 160−163°C; **FT-IR (KBr disc, υ cm^{-1}**) 3060 (Ar–H), 2950, 2892 (CH_3), 1765, 1712 (C=O), 1612 (C=N), 1550, 1514 (C=C), 1440 (N=N); **^{1}H NMR (400 MHz, DMSO-d_6) δ (ppm)** 2.26 (s, 3H), 7.52 (t, 2H, *J* = 6.0 Hz), 7.69 (dt, 2H, *J* = 6.0 & 2.4 Hz), 7.74 (dt, 2H, *J*= 6.0 & 2.4 Hz), 8.07 (t, 2H, *J* =1.1 Hz); **^{13}C NMR (100 MHz, DMSO-d_6) δ (ppm)** 16.3, 117.2, 124.7, 125.4, 128.6, 131.8, 132.2, 136.1, 137.7, 155.4, 158.6, 165.4, 178.5; **HRMS (ESI)** *m*/*z*calcd for $C_{17}H_{11}N_5O_2SNa[(M+Na)]^+$: 372.0531, found: 372.0526.

C2. 2-(4-chloro-3-((5-methyl-1,3,4-thiadiazol-2-yl)diazenyl) phenyl)-4,5,6,7-tetrahydro-1*H*-isoindole-1,3(2*H)*-dione

Yield 87%, White powder, mp 170−172°C; **FT-IR (KBr disc, υcm^{-1})** 3050 (Ar–H), 2952, 2890 (CH_3), 1760, 1705 (C=O), 1615 (C=N), 1552, 1515 (C=C), 1430 (N=N); **^{1}H NMR (400 MHz, DMSO-d_6) δ (ppm)** 2.42 (s, 3H), 7.61 (dd, 3H, *J* = 6.0 & 1.1 Hz), 7.72 (d, 2H, *J* = 6.0 Hz), 8.03 (d, 2H, *J* =1.1 Hz); **^{13}C NMR (100 MHz, DMSO-d_6) δ (ppm)** 15.2, 118.3, 123.6, 124.3, 131.2, 131.5, 131.9, 136.0, 136.6, 151.2, 157.4, 164.2, 177.4; **HRMS (ESI)** *m*/*z*calcd for $C_{17}H_{10}ClN_5O_2SNa[(M+Na)]^+$: 406.0142, found: 406.0139.

C3. 1-(3-((5-methyl-1,3,4-thiadiazol-2-yl)diazenyl)phenyl)-1*H*-pyrrole-2,5-dione

Yield 85%, Peach powder, mp 168−170°C; **FT-IR (KBr disc υ, cm^{-1}**) 3055 (Ar–H), 2945, 2895 (CH_3), 1760, 1712 (C=O), 1610 (C=N), 1548, 1515 (C=C), 1432 (N=N); **^{1}H NMR (400 MHz, DMSO-d_6) δ (ppm)** 2.28 (s, 3H), 7.51 (s, 2H), 7.54 (t, 1H, *J* = 6.0 Hz), 7.72 (dt, 1H, *J* = 6.0 & 1.1 Hz), 7.76 (dt, 1H, *J*= 6.0 & 1.1 Hz), 8.10 (t, 1H, *J* =1.1 Hz); **^{13}C NMR (100 MHz, DMSO-d_6) δ (ppm)** 15.2, 115.9, 124.7, 125.4, 126.8, 130.8, 135.7, 154.9, 157.4, 169.7, 177.4; **HRMS (ESI)** *m*/*z*calcd for $C_{13}H_9N_5O_2SNa[(M+Na)]^+$: 322.0375, found: 322.0369.

C4. 1-(4-chloro-3-((5-methyl-1,3,4-thiadiazol-2-yl)diazenyl) phenyl)-1*H*-pyrrole-2,5-dione

Yield 88%, Pale yellow powder, mp 172−174°C; **FT-IR (KBr disc υ, cm^{-1}**) 3054 (Ar–H), 2948, 2890 (CH_3), 1755, 1710 (C=O), 1610 (C=N), 1545, 1510 (C=C), 1422 (N=N); **^{1}H NMR (400 MHz, DMSO-d_6) δ (ppm)** 2.27 (s, 3H), 7.51 (s, 2H), 7.56 (d, 1H, *J* = 6.0 Hz), 7.62 (dd, 1H, *J* = 6.0 & 1.1 Hz), 8.04 (d, 1H, *J* =1.2 Hz); **^{13}C NMR (100 MHz, DMSO-d_6) δ (ppm)**15.3, 117.6, 131.3, 131.5, 132.0, 135.8, 136.9, 151.9, 157.6, 169.9, 177.5; **HRMS (ESI)** *m*/*z* calcd for $C_{13}H_8ClN_5O_2SNa[(M+Na)]^+$: 355.9985, found: 355.9987.

C5. 2-(3-((5-(4-chlorophenyl)-1,3,4-thiadiazol-2-yl)diazenyl) phenyl)-4,5,6,7-tetrahydro-1*H-isoindole-1,3*(2*H*)-*dione*

Yield 87%, Cream powder, mp 172−174°C; **FT-IR (KBr disc υ, cm^{-1}**) 3050 (Ar–H), 1762, 1718 (C=O), 1615 (C=N), 1545, 1515 (C=C), 1420 (N=N); **^{1}H NMR (400 MHz, DMSO-d_6) δ (ppm)** 7.43 (d, 2H, *J* = 6.0 Hz), 7.47–7.54 (m, 4H), 7.69 (dt, 2H, *J* = 6.0 & 1.0 Hz), 7.73 (dt, 2H, *J*= 6.0 & 1.0 Hz), 8.07 (t, 2H, *J* =1.2 Hz); **^{13}C NMR (100 MHz, DMSO-d_6) δ (ppm)**116.0, 125.0, 127.3, 127.4, 129.1, 130.7, 131.0, 131.9, 133.8, 134.3, 135.0, 136.4, 154.2, 164.1, 167.3, 177.0; **HRMS (ESI)** *m/z Calcd* for $C_{22}H_{12}ClN_5O_2SNa[(M+Na)]^+$: 468.0298, found: 468.0282.

C6. 2-(4-chloro-3-((5-(4-chlorophenyl)-1,3,4-thiadiazol-2-yl)diazenyl)phenyl) -4,5,6,7-tetrahydro-1 *H-isoindole-1,3(2H)-dione*

Yield 90%, Pale white powder, mp 168−170°C; **FT-IR (KBr disc υ, cm^{-1}**) 3045 (Ar–H), 1760, 1720 (C=O), 1605 (C=N), 1555, 1510 (C=C), 1425 (N=N); **^{1}H NMR (400 MHz, DMSO-d_6) δ (ppm)** 7.43 (d, 2H, *J* = 6.0 Hz), 7.53 (t, 5H, *J* = 5.8 Hz), 7.62 (dd, 2H, *J*= 6.0 & 1.2 Hz), 8.04 (d, 2H, *J* =1.1 Hz); **^{13}C NMR (100 MHz, DMSO-d_6) δ (ppm)** 117.9, 124.6, 127.0, 128.7, 130.8, 131.1, 131.5, 133.4, 133.9, 135.7, 136.1, 150.8, 163.7, 167.0, 176.7; **HRMS (ESI)** *m*/*z*Calcd for $C_{22}H_{11}Cl_2N_5O_2SNa[(M+Na)]^+$: 501.9909, found: 501.9901.

C7. 1-(3-((5-(4-chlorophenyl)-1,3,4-thiadiazol-2-yl)diazenyl) phenyl)-1*H-pyrrole-2,5-dione*

Yield 85%, Peach powder, mp 180−182°C; **FT-IR (KBr disc υ, cm^{-1}**) 3052 (Ar–H), 1762, 1718 (C=O), 1608 (C=N), 1550, 1510 (C=C), 1428(N=N); **^{1}H NMR (400 MHz, DMSO-d_6) δ (ppm)** 7.43 (d, 2H, *J* = 6.0 Hz), 7.49–7.52 (m, 2H), 7.53–7.55 (m, 1H), 7.69 (dt, 2H, *J* = 6.0 & 1.1 Hz), 7.74 (dt, 2H, *J*= 6.0 & 1.1 Hz), 8.08 (t, 1H, *J* =1.1 Hz); **^{13}C NMR (100 MHz, DMSO-d_6) δ (ppm)** 111.0, 121.8, 122.4, 124.1, 125.7, 125.9, 128.8, 130.7, 131.5, 149.9, 159.1, 164.7, 172.1; **HRMS (ESI)** *m*/*z*calcd for $C_{18}H_{10}ClN_5O_2SNa[(M+Na)]^+$: 418.0142, found: 418.0138.

C8. 1-(4-chloro-3-((5-(4-chlorophenyl)-1,3,4-thiadiazol-2-yl)diazenyl)phenyl)-1*H-pyrrole-2,5-dione*

Yield 87%, Light yellow powder, mp 156−158°C; **FT-IR (KBr disc υ, cm^{-1}**) 3050 (Ar–H), 1760, 1715 C=O), 1618 (C=N), 1550, 1512 (C=C), 1425 (N=N);**^{1}H NMR (400 MHz,**

DMSO-d_6) δ (ppm) 7.43 (d, 2H, J= 6.0 Hz), 7.51 (d, 3H, J= 2.8 Hz), 7.53 (d, 2H, J= 5.8 Hz), 7.63 (dd, 1H, J = 6.0 & 1.1 Hz), 8.04 (d, 1H, J = 1.1 Hz); **^{13}C NMR (100 MHz, DMSO-d_6) δ (ppm)** 117.4, 127.3, 129.1, 131.1, 131.3, 131.8, 133.8, 135.7, 136.5, 136.7, 151.7, 164.1, 169.7, 177.0; **HRMS (ESI)** m/zcalcd for $C_{18}H_9Cl_2N_5O_2SNa[(M+Na)]^+$: 451.9752, found: 451.9750.

C9. 2-(3-((5-(4-hydroxyphenyl)-1,3,4-thiadiazol-2-yl) diazenyl)phenyl)-4,5,6,7-tetrahydro-1*H-isoindole-1,3(2H)-dione*

Yield 86%, cream powder, mp 160−162°C; **FT-IR (KBr disc υ,cm^{-1})** 3420 (OH), 3045 (Ar–H), 1762,1712 (C=O), 1615 (C=N), 1550, 1515 (C=C), 1420 (N=N);**^{1}H NMR (400 MHz, DMSO-d_6) δ (ppm)** 4.07 (s, 1H), 6.91 (d, 4H, J = 5.9 Hz), 7.43 (d, 2H, J = 6.0 Hz), 7.51 (t, 1H, J= 5.8 Hz), 7.69 (dt, 1H, J = 6.0 & 1.0 Hz), 7.74 (dt, 2H, J= 6.0 & 2.4 Hz), 8.1 (t, 2H, J =1.1 Hz); **^{13}C NMR (100 MHz, DMSO-d_6) δ (ppm)** 116.9, 117.2, 126.11, 126.13, 128.4, 128.6, 131.8, 132.2, 133.0, 135.4, 155.3, 162.7, 165.2, 168.4, 178.2; **HRMS (ESI)** m/zcalcd for $C_{22}H_{13}N_5O_3SNa[(M+Na)]^+$: 450.0637, found: 450.0631.

C10. 2-(4-chloro-3-((5-(4-hydroxyphenyl)-1,3,4-thiadiazol-2-yl)diazenyl)phenyl)-4,5,6,7-tetrahydro-1 *H-isoindole-1,3(2H)-dione*

Yield 89%, White powder, mp 182−184°C; **FT-IR (KBr disc υ, cm^{-1})** 3428 (OH), 3040 (Ar-H), 1768, 1715 (C=O), 1615 (C=N), 1550, 1515 (C=C), 1430 (N=N); **^{1}H NMR (400 MHz, DMSO-d_6) δ (ppm)** 4.1 (s, 1H), 6.92 (d, 4H, J = 6.0 Hz), 7.35 (dd, 1H, J = 6.0 & 1.1 Hz), 7.44 (d, 2H, J = 6.1 Hz), 7.55 (d, 2H, J = 6.1 Hz), 7.85 (d, 2H,J = 1.1 Hz); **^{13}C NMR (100 MHz, DMSO-d_6) δ (ppm)** 116.9, 119.4, 126.11, 126.13, 128.4, 132.3, 132.6, 133.0, 135.4, 137.1, 152.3, 162.7, 165.2, 168.4, 178.2;**HRMS (ESI)** m/zcalcd for $C_{22}H_{12}ClN_5O_3SNa[(M+Na)]^+$: 484.0247, found: 484.0239.

C11. 1-(3-((5-(4-hydroxyphenyl)-1,3,4-thiadiazol-2-yl) diazenyl)phenyl)-1*H-pyrrole-2,5-dione*

Yield 90%, Peach powder, mp 172−174°C; **FT-IR (KBr disc υ,cm^{-1})** 3045 (Ar-H), 1756, 1710 (C=O), 1615 (C=N), 1545, 1510 (C=C), 1423 (N=N); **^{1}H NMR (400 MHz, DMSO-d_6) δ (ppm)** 3.57 (s, 1H), 6.69 (d, 2H, J = 5.9), 7.18 (d, 2H, J = 6.0 Hz); 7.28–7.35 (m, 3H), 7.48 (dt, 1H, J = 6.0 & 1.1 Hz), 7.55 (dt, 1H, J= 6.0 & 1.1 Hz), 7.86 (t, 1H, J =1.2 Hz); **^{13}C NMR (100 MHz, DMSO-d_6) δ (ppm)** 115.8, 115.9, 125.0, 126.8, 127.2, 130.7, 130.8, 135.7, 154.9, 161.6, 164.1, 169.7, 177.0; **HRMS (ESI)** m/zcalcd for $C_{18}H_{11}N_5O_3SNa[(M+Na)]^+$: 400.0481, found: 400.0476.

C12. 1-(4-chloro-3-((5-(4-hydroxyphenyl)-1,3,4-thiadiazol-2-yl)diazenyl)phenyl)-1 *H-pyrrole-2,5-dione*

Yield 87%, Pale yellow powder, mp 162 − 164°C; **FT-IR (KBr disc υ, cm^{-1})** 3410 (OH), 3035 (Ar–H), 1755, 1710 (C=O), 1615 (C=N), 1545, 1515 (C=C), 1425 (N=N); **^{1}H NMR (400 MHz, DMSO-d_6) δ (ppm)** 4.07 (s, 1H), 6.91 (d, 2H, J = 6.0 Hz), 7.43 (d, 2H, J = 6.0), 7.51 (s, 2H), 7.54 (d, 1H, J = 6.0 Hz), 7.62 (dd, 1H, J = 6.0 & 1.2 Hz), 8.04 (d, 1H,J = 1.1 Hz); **^{13}C NMR (100 MHz, DMSO-d_6) δ (ppm)** 115.8, 117.4, 125.0, 127.2, 131.1, 131.3, 131.8, 135.7, 136.7, 151.7, 161.6, 164.1, 169.7, 177.0; **HRMS (ESI)** m/zcalcd for $C_{18}H_{10}ClN_5O_3SNa[(M+Na)]^+$: 434.0091, found: 434.0088.

C13. 2-(3-((5-(4-nitrophenyl)-1,3,4-thiadiazol-2-yl)diazenyl) phenyl) -4,5,6,7-tetrahydro-1*H-isoindole-1,3(2H)-dione*

Yield 88%, Pale white powder, mp 110−112°C; **FT-IR (KBr disc υ,cm^{-1})** 3050 (Ar–H), 1765, 1720 (C=O), 1605 (C=N), 1545, 1512 (C=C), 1540, 1344 (NO_2), 1435 (N=N); **^{1}H NMR (400 MHz, DMSO-d_6) δ (ppm)** 7.52 (t, 2H, J = 6.0 Hz), 7.68 (dt, 2H, J = 6.0 & 1.2 Hz), 7.73 (dt, 1H, J= 6.0 & 1.1 Hz), 7.83 (d, 3H, J = 6.0 Hz), 8.08 (t, 2H, J =1.1 Hz), 8.29 (d, 2H, J= 6.0 Hz); **^{13}C NMR (100 MHz, DMSO-d_6) δ (ppm)** 117.1, 125.2, 126.0, 127.8, 128.5, 131.7, 132.1, 132.9, 135.3, 136.0, 140.5, 148.4, 155.2, 165.2, 168.4, 178.1; **HRMS (ESI)** m/zcalcd for $C_{22}H_{12}N_6O_4SNa[(M+Na)]^+$: 479.0539, found: 479.0528.

C14. 2-(4-chloro-3-((5-(4-nitrophenyl)-1,3,4-thiadiazol-2-yl) diazenyl)phenyl)-4,5,6,7-tetrahydro-1 *H-isoindole-1,3(2H)-dione*

Yield 87%, Pale white powder, mp 114−116°C; **FT-IR (KBr disc υ,cm^{-1})** 3052 (Ar–H), 1762, 1718 (C=O), 1608 (C=N), 1540, 1520 (C=C), 1535, 1345 (NO_2), 1438 (N=N); **^{1}H NMR (400 MHz, DMSO-d_6) δ (ppm)** 7.53 (d, 2H, J = 6.0 Hz), 7.63 (dd, 2H, J = 6.0 & 1.1 Hz), 7.83 (d, 3H, J= 6.0 Hz), 8.05 (d, 2H, J =1.2 Hz), 8.29 (d, 2H, J= 6.0 Hz); **^{13}C NMR (100 MHz, DMSO-d_6) δ (ppm)** 118.5, 124.4, 125.2, 126.9, 131.4, 131.7, 132.1, 134.5, 136.3, 139.7, 147.6, 151.4, 164.4, 167.6, 177.3; **HRMS (ESI)** m/zcalcd for $C_{22}H_{11}ClN_6O_4SNa[(M+Na)]^+$: 513.0149, found: 513.0138.

C15. 1-(3-((5-(4-nitrophenyl)-1,3,4-thiadiazol-2-yl)diazenyl) phenyl)-1*H -pyrrole-2,5-dione*

Yield 85%, Pale yellow powder, mp 150−152°C; **FT-IR (KBr disc υ,cm^{-1})** 3055 (Ar–H), 1760, 1715 (C=O), 1618 (C=N), 1545, 1522 (C=C), 1536, 1342 (NO_2), 1435 (N=N);**^{1}H NMR (400 MHz, DMSO-d_6) δ (ppm)** 7.47–7.55 (m, 3H), 7.68 (dt, 1H, J = 6.0 & 1.2 Hz), 7.75 (dt, 1H, J= 6.0

& 1.1 Hz), 7.80 (d, 2H, J = 6.0 Hz), 8.06 (t, 1H, J =1.2 Hz), 8.28 (d, 2H, J= 6.1 Hz); **^{13}C NMR (100 MHz, DMSO-d_6) δ (ppm)** 115.9, 124.2, 126.7, 126.8, 130.8, 135.66, 135.70, 139.4, 147.4, 154.9, 164.1, 169.7, 177.0; **HRMS (ESI)** m/zcalcd for $C_{18}H_{10}N_6O_4SNa[(M+Na)]^+$: 429.0382, found: 429.0378.

C16. 1-(4-chloro-3-((5-(4-nitrophenyl)-1,3,4-thiadiazol-2-yl)diazenyl)phenyl)-1*H-pyrrole-2,5-dione*

Yield 82%, Cream powder, mp 146−148°C; **FT-IR (KBr disc υ,cm^{-1})** 3050 (Ar-H), 1758, 1712 (C=O), 1618 (C=N), 1548, 1525 (C=C), 1532, 1347 (NO_2), 1422 (N=N); **^{1}H NMR (400 MHz, DMSO-d_6) δ (ppm)** 7.51 (s, 2H), 7.52–7.56 (m, 2H), 7.84 (d, 2H, J = 6.0), 8.16 (d, 1H, J = 1.0 Hz), 8.29 (d, 2H,J = 6.0 Hz); **^{13}C NMR (100 MHz, DMSO-d_6) δ (ppm)** 119.3, 126.0, 128.6, 133.0, 133.2, 133.7, 137.5, 138.6, 141.3, 149.3, 153.6, 166.0, 171.6, 178.9; **HRMS (ESI)** m/z calcd for $C_{18}H_9ClN_6O_4SNa[(M+Na)]^+$: 462.9993, found: 462.9990.

C17. 2-(3-((5-(4-chlorophenyl)-1,3,4-oxadiazol-2-yl) diazenyl)phenyl)-4,5,6,7-tetrahydro-1*H-isoindole-1,3(2H)-dione*

Yield 87%, Light brown powder, mp 180−182°C; **FT-IR (KBr disc υ, cm^{-1})** 3055 (Ar–H), 1765, 1722 (C=O), 1615 (C=N), 1545, 1525 (C=C), 1435 (N=N); **^{1}H NMR (400 MHz, DMSO-d_6) δ (ppm)** 7.43 (d, 4H, J = 6.0 Hz), 7.48–7.56 (m, 3H), 7.68 (dt, 1H, J = 6.0 & 1.0 Hz), 7.73 (dt, 2H, J= 6.0 & 1.0 Hz), 8.08 (t, 2H, J =1.2 Hz); **^{13}C NMR (100 MHz, DMSO-d_6) δ (ppm)** 117.8, 126.7, 129.2, 129.8, 130.1, 131.2, 132.4, 132.8, 133.6, 136.0, 136.7, 139.0, 155.9, 156.0, 169.1, 171.4; **HRMS (ESI)**m/zcalcd for $C_{22}H_{12}ClN_5O_3Na[(M+Na)]^+$: 452.0527, found: 452.0521.

C18. 2-(4-chloro-3-((5-(4-chlorophenyl)-1,3,4-oxadiazol-2-yl)diazenyl)phenyl)-4,5,6,7-tetrahydro-1 *H-isoindole-1,3(2H)-dione*

Yield 90%, White powder, mp 188–190°C; **FT-IR (KBr disc υ,cm^{-1})** 3055 (Ar–H), 1758, 1710 (C=O), 1606 (C=N), 1545, 1525 (C=C), 1436 (N=N);**^{1}H NMR (400 MHz, DMSO-d_6) δ (ppm)** 7.41 (d, 4H, J = 6.0 Hz), 7.49 (s, 1H), 7.51 (t, 2H, J = 5.8 Hz), 7.61 (dd, 2H, J= 6.0 & 1.2 Hz), 8.04 (d, 2H, J =1.1 Hz); **^{13}C NMR (100 MHz, DMSO-d_6) δ (ppm)** 118.2, 124.9, 128.0, 128.3, 129.4, 131.1, 131.4, 131.8, 134.2, 136.0, 137.2, 151.1, 154.2, 167.2, 169.6; **HRMS (ESI)** m/zcalcd for $C_{22}H_{11}Cl_2N_5O_3Na[(M+Na)]^+$: 486.0137, found: 486.0126.

C19. *1-(3-((5-(4-chlorophenyl)-1,3,4-oxadiazol-2-yl) diazenyl)phenyl)-1H-pyrrole-2,5-dione*

Yield 85%, Cream powder, mp 178−180°C; **FT-IR (KBr disc υ,cm^{-1})** 3030 (Ar–H), 1752, 1708 (C=O), 1610 (C=N), 1545, 1512 (C=C), 1422 (N=N); **^{1}H NMR (400 MHz, DMSO-d_6) δ (ppm)** 7.43 (d, 2H, J = 6.0 Hz), 7.49–7.54 (m, 5H), 7.69 (dt, 1H, J = 6.0 & 1.1 Hz), 7.73 (dt, 1H, J= 6.0 & 1.1 Hz), 8.07 (t, 1H, J =1.1 Hz); **^{13}C NMR (100 MHz, DMSO-d_6) δ (ppm)** 116.0, 126.8, 128.1, 128.4, 129.4, 130.7, 130.8, 135.66, 135.70, 137.3, 154.3, 154.9, 169.67, 169.70; **HRMS (ESI)** m/zcalcd for $C_{18}H_{10}ClN_5O_3Na[(M+Na)]^+$: 402.0370, found: 402.0365.

C20. 1-(4-chloro-3-((5-(4-chlorophenyl)-1,3,4-oxadiazol-2-yl)diazenyl)phenyl)-1*H-pyrrole-2,5-dione*

Yield 85%, Light yellow powder, mp 148−150°C; **FT-IR (KBr disc υ,cm^{-1})** 3035 (Ar–H), 1755, 1710 (C=O), 1615 (C=N), 1545, 1515 (C=C), 1425 (N=N);**^{1}H NMR (400 MHz, DMSO-d_6) δ (ppm)**7.43 (d, 2H, J= 6.0 Hz), 7.49–7.55 (m, 5H), 7.62 (dd, 1H, J = 6.0 & 1.1 Hz), 8.04 (d, 1H, J = 1.1 Hz); **^{13}C NMR (100 MHz, DMSO-d_6) δ (ppm)** 117.2, 127.8, 128.1, 129.2, 130.8, 131.1, 131.6, 135.4, 136.5, 137.0, 151.5, 154.0, 169.42, 169.45; **HRMS (ESI)** m/zcalcd for $C_{18}H_9Cl_2N_5O_3Na[(M+Na)]^+$: 435.9980, found: 435.9950.

C21. 2-(3-((5-(4-hydroxyphenyl)-1,3,4-oxadiazol-2-yl) diazenyl)phenyl)-4,5,6,7-tetrahydro-1 *H-isoindole-1, 3(2H)-dione*

Yield 87%, Light yellow powder, mp 166−168°C; **FT-IR (KBr disc υ,cm^{-1})** 3425 (OH), 3050 (Ar–H), 1770, 1715 (C=O), 1618 (C=N), 1550, 1512 (C=C), 1435 (N=N); **^{1}H NMR (400 MHz, DMSO-d_6) δ (ppm)**3.98 (s, 1H), 6.80 (d, 4H, J = 6.0 Hz), 7.31 (d, 2H, J = 6.0 Hz), 7.42 (t, 1H, J = 6.0 Hz); 7.59 (dt, 1H, J = 6.0 & 1.0 Hz), 7.63 (dt, 2H, J= 6.0 & 2.4 Hz), 7.98 (t, 2H, J =1.1 Hz); **^{13}C NMR (100 MHz, DMSO-d_6) δ (ppm)** 115.8, 116.0, 117.4, 125.0, 127.4, 127.6, 130.7, 131.0, 131.9, 134.3, 135.0, 154.2, 154.3, 160.8, 167.3, 169.7; **HRMS (ESI)** m/zcalcd for $C_{22}H_{13}N_5O_4Na[(M+Na)]^+$: 434.0866, found: 434.0859.

C22. 2-(4-chloro-3-((5-(4-hydroxyphenyl)-1,3,4-oxadiazol-2-yl)diazenyl)phenyl)-4,5,6,7-tetrahydro-1*H-isoindole-1,3(2H)-dione*

Yield 89%, Light yellow powder, mp 176−178°C; **FT-IR (KBr disc υ,cm^{-1})** 3420 (OH), 3045 (Ar–H), 1765, 1710 (C=O), 1605 (C=N), 1545, 1518 (C=C), 1440 (N=N); **^{1}H NMR (400 MHz, DMSO-d_6) δ (ppm)**3.98 (s, 1H), 6.82 (d, 4H, J = 6.0 Hz), 7.32 (d, 2H, J = 6.0 Hz), 7.44 (d, 1H, J = 6.1 Hz), 7.52 (dd, 2H, J = 6.1 & 1.1 Hz), 7.94 (d, 2H,J = 1.1 Hz);

^{13}C NMR (100 MHz, DMSO-d_6) δ (ppm) 115.8, 117.4, 118.3, 125.0, 127.6, 131.2, 131.5, 131.9, 134.3, 136.0, 151.2, 154.3, 160.8, 167.3, 169.7; **HRMS (ESI)** m/zcalcd for $C_{22}H_{10}ClN_5O_4Na[(M+Na)]^+$: 468.0476, found: 468.0463.

C23. 1-(3-((5-(4-hydroxyphenyl)-1,3,4-oxadiazol-2-yl) diazenyl)phenyl)-1*H-pyrrole-2,5-dione*

Yield 85%, Yellow powder, mp 160−162°C; **FT-IR (KBr disc υ,cm^{-1})** 3418 (OH), 3050 (Ar–H), 1752, 1705 (C=O), 1614 (C=N), 1545, 1510 (C=C), 1420 (N=N); **^{1}H NMR (400 MHz, DMSO-d_6) δ (ppm)** 4.17 (s, 1H), 6.99 (d, 2H, J = 6.0), 7.49 (d, 2H, J = 6.0 Hz); 7.55–7.65 (m, 3H), 7.77 (dt, 1H, J = 6.0 & 1.1 Hz), 7.82 (dt, 1H, J= 6.0 & 1.1 Hz), 8.16 (t, 1H, J =1.2 Hz); **^{13}C NMR (100 MHz, DMSO-d_6) δ (ppm)** 115.8, 115.9, 117.4, 126.8, 127.6, 130.7, 130.8, 135.66, 135.70, 154.3, 154.9, 160.8, 169.67, 169.70; **HRMS (ESI)** m/zcalcd for $C_{18}H_{11}N_5O_4Na[(M+Na)]^+$: 384.0709, found: 384.0701.

C24. 1-(4-chloro-3-((5-(4-hydroxyphenyl)-1,3,4-oxadiazol-2-yl)diazenyl)phenyl)-1*H-pyrrole-2,5-dione*

Yield 82%, Yellow powder, mp 152−154°C; **FT-IR (KBr disc υ, cm^{-1})** 3425 (OH), 3045 (Ar–H), 1762, 1715 (C=O), 1612 (C=N), 1545, 1514 (C=C), 1422 (N=N); **^{1}H NMR (400 MHz, DMSO-d_6) δ (ppm)** 4.60 (s, 1H), 7.38 (d, 2H, J = 6.0 Hz), 7.88 (d, 2H, J = 6.0), 7.98 (s, 2H), 8.01 (d, 1H, J = 6.0 Hz), 8.09 (dd, 1H, J = 6.0 & 1.2 Hz), 8.51 (d, 1H,J = 1.1 Hz); **^{13}C NMR (100 MHz, DMSO-d_6) δ (ppm)** 116.1, 117.70, 117.72, 127.9, 131.4, 131.6, 132.1, 136.0, 137.0, 152.0, 154.6, 161.1, 169.96, 169.99;

HRMS (ESI) m/zcalcd for $C_{18}H_{10}ClN_5O_4Na[(M+Na)]^+$: 418.0319, found: 418.0316.

C25. 2-(3-((5-(4-nitrophenyl)-1,3,4-oxadiazol-2-yl)diazenyl) phenyl)-4,5,6,7-tetrahydro-1 *H-isoindole-1,3(2H)-dione*

Yield 85%, Pale yellow powder, mp 200−202°C; **FT-IR (KBr disc υ,cm^{-1})** 3050 (Ar–H), 1765, 1722 (C=O), 1615 (C=N), 1550, 1512 (C=C), 1532, 1345 (NO_2), 1435 (N=N); **^{1}H NMR (400 MHz, DMSO-d_6) δ (ppm)** 7.53 (t, 2H, J = 6.0 Hz), 7.70 (dt, 2H, J = 6.0 & 1.2 Hz), 7.75 (dt, 2H, J= 6.0 & 1.1 Hz), 7.83 (d, 2H, J = 6.0 Hz), 8.10 (t, 2H, J =1.1 Hz), 8.31 (d, 2H, J= 6.0 Hz); **^{13}C NMR (100 MHz, DMSO-d_6) δ (ppm)** 116.0, 124.7, 125.0, 127.4, 130.7, 131.0, 131.9, 132.1, 134.3, 135.0, 147.4, 154.2, 154.3, 167.3, 169.7; **HRMS (ESI)** m/zcalcd for $C_{22}H_{12}N_6O_5Na[(M+Na)]^+$: 463.0767, found: 463.0755.

C26. 2-(4-chloro-3-((5-(4-nitrophenyl)-1,3,4-oxadiazol-2-yl)diazenyl)phenyl)-4,5,6,7-tetrahydro-1 *H-isoindole-1, 3(2H)-dione*

Yield 90%, Yellow powder, mp 184−186°C; **FT-IR (KBr disc υ,cm^{-1})** 3030 (Ar–H), 1770, 1715 (C=O), 1612 (C=N), 1550, 1515 (C=C), 1535, 1347 (NO_2), 1432 (N=N);**^{1}H NMR (400 MHz, DMSO-d_6) δ (ppm)** 7.54 (d, 4H, J = 6.0 Hz), 7.63 (dd, 1H, J = 6.0 & 1.1 Hz), 7.84 (d, 2H, J= 6.0 Hz), 8.05 (d, 2H, J =1.2 Hz), 8.30 (d, 2H, J= 6.0 Hz); **^{13}C NMR (100 MHz, DMSO-d_6) δ (ppm)** 119.0, 125.4, 125.7, 128.2, 131.9, 132.2, 132.6, 132.8, 135.0, 136.7, 148.1, 151.9, 155.0, 168.0, 170.4; **HRMS (ESI)** m/zcalcd for $C_{22}H_{11}ClN_6O_5Na[(M+Na)]^+$: 497.0377, found: 497.0369.

C27. 1-(3-((5-(4-nitrophenyl)-1,3,4-oxadiazol-2-yl) diazenyl)phenyl)-1*H-pyrrole-2,5-dione*

Yield 85%, Yellow powder, mp 230−232°C; **FT-IR (KBr disc υ,cm^{-1})** 3055 (Ar–H), 1752, 1709 (C=O), 1606 (C=N), 1545, 1502 (C=C), 1535, 1340 (NO_2), 1425 (N=N); **^{1}H NMR (400 MHz, DMSO-d_6) δ (ppm)** 7.52–7.57 (m, 3H), 7.72 (dt, 1H, J = 6.0 & 1.2 Hz), 7.77 (dt, 1H, J= 6.0 & 1.1 Hz), 7.85 (d, 2H, J = 6.0 Hz), 8.10 (t, 1H, J =1.2 Hz), 8.32 (d, 2H, J= 6.1 Hz); **^{13}C NMR (100 MHz, DMSO-d_6) δ (ppm)** 118.2, 126.9, 129.0, 129.6, 132.9, 133.0, 134.3, 137.87, 137.90, 149.6, 156.5, 157.1, 171.9; **HRMS (ESI)** m/zcalcd for $C_{18}H_{10}N_6O_5Na[(M+Na)]^+$: 413.0611, found: 413.0609.

C28. 1-(4-chloro-3-((5-(4-nitrophenyl)-1,3,4-oxadiazol-2-yl)diazenyl)phenyl)-1 *H -pyrrole-2, 5-dione*

Yield 89%, Yellow powder, mp 192−194°C; **FT-IR (KBr disc υ,cm^{-1})** 3035 (Ar–H), 1750, 1709 (C=O), 1612 (C=N), 1542 (C=C), 1530, 1345 (NO_2), 1420 (N=N);**^{1}H NMR (400 MHz, DMSO-d_6) δ (ppm)** 7.43–7.51 (m, 3H), 7.56 (dd, 1H, J = 6.0 & 1.1 Hz), 7.76 (d, 2H, J = 6.0 Hz), 7.98 (d, 1H, J = 1.0 Hz), 8.24 (d, 2H, J = 6.0 Hz); **^{13}C NMR (100 MHz, DMSO-d_6) δ (ppm)** 117.4, 124.7 127.4, 131.1, 131.3, 131.8, 132.1, 135.7, 136.7, 147.4, 151.7, 154.3, 169.7; **HRMS (ESI)** m/zcalcd for $C_{18}H_9ClN_6O_6Na[(M+Na)]^+$: 447.0220, found: 447.0216.

Pharmacology

Cell culture

Human breast cancer cell line MCF-7 (adenocarcinoma) and HT-29 (colorectal adenocarcinoma) were used in this study. Both the cell lines were procured from the repository of National Centre of Cellular Sciences (NCCS), Pune, India. These cells were cultured in the Dulbecco's modified Eagle's

medium (DMEM, Sigma-Aldrich, India) at pH 7.4, supplemented with 10 % heat-activated foetal bovine serum (FBS), 5 μM ciprofloxacin and 40 μM Gentamicin in a humidified incubator at 37 ±0.5°C under 5 % CO_2 atmosphere.

MTT assay

The synthesized compounds (**C1-C28**) were evaluated for their cytotoxicity (or viability) against human cancer cell lines (MCF-7 and HT-29) by 3-(4,5-dimethylthiazol-2-yl)-2,5-diphenyltetrazolium bromide (MTT) assay [38]. Doxorubicin was used as a reference drug, and standard protocol was followed [38]. Cancer cells maintained in appropriate conditions were placed in 96-well plates ($1x10^4$ cells/well) and incubated with DMEM containing five different concentrations of compounds, i.e., 10, 1, 0.1, 0.01 and 0.001 μM, at 37°C, 5% CO_2 for 96 h. After that 20 μl of MTT reagent was added (0.5 mg/mL) to the medium and incubated for next 4 h. The dark blue formazan crystals were dissolved in DMSO, and the absorbance was measured using an ELISA micro-plate reader at 550 nm. The results are determined as percentage inhibitions and calculated according to the following equation.

% Inhibition = control–test/control × 100,

where 'control' was the absorbance of the control (without compound) and 'test' was the absorbance in the presence of the compound.

All tests were performed in triplicate, and IC_{50} values for compounds were calculated from the concentration–response curves by means of the PRISM 4.0 (GraphPad Software) [39].

Molecular docking

Potential targets (target fishing) were identified using ChemMapper server [23]. The core structure (in smile format) was submitted to web server, where it was screened against PDB (7,072 entries) using a 3D similarity-based SHAFTS method. Two PDB entries with id 2R3J [40] and 2J5F [41] were among the top 10 (3^{rd} and 7^{th}, respectively) scored with well-documented literature as validated targets in cancer therapy. These two proteins were then docked against top three scorers of each cell line (based on MTT assays).

For our docking study, the crystal structure of cyclin-dependent kinase 2 (PDB ID: 2R3J) and that of EGFR kinase domain of tyrosine kinase (PDB ID: 2J5F) were obtained from the Protein Data Bank (RCSB-PDB). Both of the proteins play a crucial role in the maintenance of genomic integrity and cellular proliferation.

Molecular docking study was performed using AutoDock 4.2 suite, an automated docking tool that uses Lamarckian genetic algorithm (LGA) [42]. Protein structures were cleaned by removing crystallographic water, bound substrates and co-factors. Polar hydrogen atoms were added, and Gasteiger charges were computed in ADT [30]. 2D structures of all ligands were drawn using ChemDraw ultra 12.0 (www.cambridgesoft.com) and were converted to 3D. Finally, all the structures were energy-minimized and geometrically optimized using AM1 (Austin Model 1) force field. Prior to extensive docking experiments, validity/robustness of the docking engine (i.e., AutoDock 4.2) was judged by control docking/self-docking experiment. For this purpose, co-crystallized ligands were first removed from the protein structure and then re-docked again. The drug-likeness of the synthesized compounds was also evaluated using Molinspiration property calculation service [34].

In the docking process the grid points were fixed at a distance of 0.375Å with the grid box of size 66 × 66 × 84 (number of points in x-, y- and z-axis for both proteins). Default parameters were used for docking run (number of final conformations: 10, population size: 150, maximum number of energy evaluations: 2.5×10^6 and maximum number of generations: 27000). All docked poses were inspected in detail for their binding interactions with binding cavity of the target protein, using two visualizing tools Discovery Studio Visualizer (DSV) [31] and Molegro Molecular Viewer (MMV) [32]. File formats were changed using Open Babel toolbox [44] (see supporting information for more detail).

Acknowledgements The authors are thankful to the GITAM University, IIT Roorkee and Andhra University for providing instrumental facility. This research was supported by funds from University Grants Commission (UGC, Government of India) [F. No. 42-239/2013 (SR)]. We sincerely extend our gratitude to Deshpande Laboratories Pvt. Ltd. for performing anticancer studies.

Compliance with ethical standards

Conflict of interest The authors report no conflicts of interest in this work.

References

1. Siegel RL, Miller KD, Jemal A (2016) Cancer statistics, 2016. CA: Cancer J Clin 66:7–30. https://doi.org/10.3322/caac.21332
2. Jemal A, Center MM, DeSantis C, Ward EM (2010) Global patterns of cancer incidence and mortality rates and trends. Cancer Epidemiol Biomark Prev 19:1893–1907. https://doi.org/10.1158/1055-9965.EPI-10-0437
3. Garraway LA, Jänne PA (2012) Circumventing cancer drug resistance in the era of personalized medicine. Cancer Discov 2:215–226. https://doi.org/10.1158/2159-8290.CD-12-0012
4. Iwamoto T (2013) Clinical application of drug delivery systems in cancer chemotherapy: review of the efficacy and side effects of approved drugs. Biol Pharm Bull 36:715–718. https://doi.org/10.1248/bpb.b12-01102
5. Monsuez J-J, Charniot J-C, Vignat N, Artigou J-Y (2010) Cardiac side-effects of cancer chemotherapy. Int J Cardiol 144:3–15. https://doi.org/10.1016/j.ijcard.2010.03.003

6. Faden RR, Chalkidou K, Appleby J, Waters HR, Leider JP (2009) Expensive cancer drugs: a comparison between the United States and the United Kingdom. Milbank Q 87:789–819. https://doi.org/10.1111/j.1468-0009.2009.00579.x
7. Bach PB (2009) Limits on medicare's ability to control rising spending on cancer drugs. N Engl J Med 360:626–633. https://doi.org/10.1056/NEJMhpr0807774
8. Gibbs JB (2000) Mechanism-based target identification and drug discovery in cancer research. Science 287:1969–1973. https://doi.org/10.1126/science.287.5460.1969
9. Vogelstein B, Kinzler K (2004) Cancer genes and the pathways they control. Nat Med 10:789–799. https://doi.org/10.1038/nm1087
10. Neidle S, Thurston DE (2005) Chemical approaches to the discovery and development of cancer therapies. Nat Rev Cancer 5:285–296. https://doi.org/10.1038/nrc1587
11. Muregi FW, Ishih A (2010) Next-generation antimalarial drugs: hybrid molecules as a new strategy in drug design. 71:20–32. https://doi.org/10.1002/ddr.20345
12. N'soukpoé-Kossi CN, Descôteaux C, Asselin É, Tajmir-Riahi H-A, Bérubé G (2008) DNA interaction with novel antitumor estradiol-platinum(II) hybrid molecule: a comparative study with cisplatin drug. DNA Cell Biol 27:101–107. https://doi.org/10.1089/dna.2007.0669
13. Solomon VR, Hu C, Lee H (2009) Hybrid pharmacophore design and synthesis of isatin-benzothiazole analogs for their anti-breast cancer activity. Bioorganic Med Chem 17:7585–7592. https://doi.org/10.1016/j.bmc.2009.08.068
14. Solomon VR, Hu C, Lee H (2010) Design and synthesis of anti-breast cancer agents from 4-piperazinylquinoline: a hybrid pharmacophore approach. Bioorganic Med Chem 18:1563–1572. https://doi.org/10.1016/j.bmc.2010.01.001
15. Sashidhara KV, Kumar A, Kumar M, Sarkar J, Sinha S (2010) Synthesis and in vitro evaluation of novel coumarin-chalcone hybrids as potential anticancer agents. Bioorganic Med Chem Lett 20:7205–7211. https://doi.org/10.1016/j.bmcl.2010.10.116
16. Teiten M-H, Dicato M, Diederich M (2014) Hybrid Curcumin compounds: a new strategy for cancer treatment. Molecules 19:20839–20863. https://doi.org/10.3390/molecules191220839
17. Nepali K, Sharma S, Sharma M, Bedi PMS, Dhar KL (2014) Rational approaches, design strategies, structure activity relationship and mechanistic insights for anticancer hybrids. Eur J Med Chem 77:422–487. https://doi.org/10.1016/j.ejmech.2014.03.018
18. Jain AK, Sharma S, Vaidya A, Ravichandran V, Agrawal RK (2013) 1,3,4-thiadiazole and its derivatives: a review on recent progress in biological activities. Chem Biol Drug Des 81:557–576. https://doi.org/10.1111/cbdd.12125
19. Taher AT, Georgey HH, El-Subbagh HI (2012) Novel 1,3,4-heterodiazole analogues: synthesis and in- vitroantitumor activity. Eur J Med Chem 47:445–451. https://doi.org/10.1016/j.ejmech.2011.11.013
20. Sondhi SM, Rani R, Roy P, Agrawal SK, Saxena AK (2009) Microwave-assisted synthesis of N-substituted cyclic imides and their evaluation for anticancer and anti-inflammatory activities. Bioorganic Med Chem Lett 19:1534–1538. https://doi.org/10.1016/j.bmcl.2008.07.048
21. Kok SHL et al (2008) Synthesis and anti-cancer activity of benzothiazole containing phthalimide on human carcinoma cell lines. Bioorganic Med Chem 16:3626–3631. https://doi.org/10.1016/j.bmc.2008.02.005
22. Miyachi H, Ogasawara A, Azuma A, Hashimoto Y (1997) Tumor necrosis factor-alpha production-inhibiting activity of phthalimide analogues on human leukemia THP-1 cells and a structure-activity relationship study. Bioorganic Med Chem 5:2095–2102. https://doi.org/10.1016/S0968-0896(97)00148-X
23. Gong J, Cai C, Liu X, Ku X, Jiang H, Gao D, Li H (2013) ChemMapper: a versatile web server for exploring pharmacology and chemical structure association based on molecular 3D similarity method. Bioinformatics 29:1827–1829. https://doi.org/10.1093/bioinformatics/btt270
24. Berman HM, Westbrook J, Feng Z, Gilliland G, Bhat TN, Weissig H, Shindyalov IN, Bourne PE (2000) The protein data bank. Nucleic Acids Res 28:235–242. https://www.ncbi.nlm.nih.gov/pmc/articles/PMC102472/
25. Sairam KV, Gurupadyya BM, Vishwanathan BI, Chandan RS, Nagesha D (2016) Cytotoxicity studies of coumarin analogs: design, synthesis and biological activity. RSC Adv 6:98816–98828. https://doi.org/10.1039/C6RA22466K
26. Paarakh PM, Sreeram DC, D SS, Ganapathy SPS (2015) In vitro cytotoxic and in silico activity of piperine isolated from piper nigrum fruits Linn. In Silico Pharmacol 3:9–15. https://doi.org/10.1186/s40203-015-0013-2
27. Aboul-Fadl T, Radwan AA, Attia MI, Al-Dhfyan A, Abdel-Aziz HA (2012) Schiff bases of indoline-2,3-dione (isatin) with potential antiproliferative activity. Chem Cent J 6:49–59. https://doi.org/10.1186/1752-153X-6-49
28. Pawar VG, Sos ML, Rode HB, Rabiller M, Heynck S, van Otterlo WA, Thomas RK, Rauh D (2010) Synthesis and biological evaluation of 4-anilinoquinolines as potent inhibitors of epidermal growth factor receptor. J Med Chem 53:2892–2901. https://doi.org/10.1021/jm901877j
29. Yadav DK, Rai R, Kumar N, Singh S, Misra S, Sharma P, Shaw P, Pérez-Sánchez H, Mancera RL, Choi EH, Kim MH, Pratap R (2016) New arylated benzo[h]quinolines induce anticancer activity by oxidative stress-mediated DNA damage. Sci Rep 6:38128–381140. https://doi.org/10.1038/srep38128
30. Morris GM, Huey R, Lindstrom W, Sanner MF, Belew RK, Goodsell DS, Oslon AJ (2009) AutoDock4 and AutoDockTools4: automated docking with selective receptor flexibility. J Comput Chem 16:2785–2791. https://doi.org/10.1002/jcc.21256
31. Dassault Systèmes BIOVIA, Discovery studio visualizer, Release 2017, San Diego: Dassault Systèmes, 2016. http://accelrys.com/products/collaborative-science/biovia-discovery-studio/visualization.html . Accessed 12 Dec 2017
32. Thomsen R, Christensen MH (2006) MolDock: a new technique for high-accuracy molecular docking. J Med Chem 49:3315–3321. https://doi.org/10.1021/jm051197e
33. Lipinski CA (2004) Lead- and drug-like compounds: the rule-of-five revolution. Drug Discov Today Technol 1:337–341. https://doi.org/10.1016/j.ddtec.2004.11.007
34. Lajiness MS, Vieth M, Erickson J (2004) Molecular properties that influence oral drug—like behaviour. Curr Opin Drug Discov Devel 7:470–477. https://www.ncbi.nlm.nih.gov/pubmed/15338956
35. Leeson PD, Springthorpe B (2007) The influence of drug-like concepts on decision-making in medicinal chemistry. Nat Rev Drug Discov 6:881–890
36. Vamecq J, Bac P, Herrenknecht C, Maurois P, Delcourt P, Stables JP (2000) Synthesis and anticonvulsant and neurotoxic properties of substituted *N*-phenyl derivatives of the phthalimide pharmacophore. J Med Chem 43:1311–1319. https://doi.org/10.1021/jm990068t
37. Collin X, Robert J-M, Wielgosz G, Baut GL, Bobin-Dubigeon C, Grimaud N, Petit J-Y (2001) New anti-inflammatory *N*-pyridinyl(alkyl)phthalimides acting as tumour necrosis factor-α production inhibitors. Eur J Med Chem 36:639–649. https://doi.org/10.1016/S0223-5234(01)01254-5
38. Meerloo Jv, Kaspers GJL, Cloos J (2011) Cell sensitivity assays: the MTT Assay. In: Cree I (eds) Cancer cell culture. methods in molecular biology (Methods and Protocols), 731. Humana Press. https://doi.org/10.1385/1-59259-406-9:165
39. GraphPad Software, La Jolla California USA. https://doi.orgwww.graphpad.com

40. Fischmann TO, Hruza A, Duca JS, Ramanathan L, Mayhood T, Windsor WT, Le HV, Guzi TJ, Dwyer MP, Paruch K, Doll RJ, Lees E, Parry D, Seghezzi W, Madison V (2008) Structure-guided discovery of cyclin-dependent kinase inhibitors. Biopolymers 89:372–379. https://doi.org/10.1002/bip.20868
41. Blair JA, Rauh D, Kung C, Yun C-H, Fan Q-W, Rode H, Zhang C, Eck MJ, Weiss WA, Shokat KM (2007) Structure-guided development of affinity probes for tyrosine kinases using chemical genetics. Nat Chem Biol 3:229–238. https://doi.org/10.1038/nchembio866
42. Garrett MM, Goodsell DS, Halliday RS, Huey R, Hart WE, Belew RK, Oslon AJ (1998) Automated docking using a Lamarckian genetic algorithm and an empirical binding free energy function. J Comput Chem 19:1639–1662. https://doi.org/10.1002/(SICI)1096-987X(19981115)19:14<1639::AID-JCC10>3.0.CO;2-B
43. Molinspiration Cheminformatics, Bratislava, Slovak Republic. http://www.molinspiration.com/services/properties.html. Accessed Dec 20
44. O'Boyle NM, Banck M, James CA, Morley CA, Vandermeersch T, Hutchison GR (2011) Open Babel: an open chemical toolbox. J Cheminform 3:1–14. https://doi.org/10.1186/1758-2946-3-33